Int. J. Multiphase Flow Vol. 7, pp. 439–460, 1981
Printed in Great Britain.

0301-9322/81/040439-22$02.00/0
Pergamon/Elsevier

CHARACTERISTICS OF LASER-DOPPLER SIGNALS FROM BUBBLES

W. W. MARTIN and A. H. ADBELMESSIH
Department of Mechanical Engineering, University of Toronto, Toronto, Canada

and

J. J. LISKA and F. DURST
Sonderforschungsbereich 80, Universität Karlsruhe, Kaiserstrasse 12, D-7500 Karlsruhe 1, F.R.G.

(*Received* 4 *March* 1980; *in revised form* 2 *December* 1980)

Abstract—The present paper concerns the application of laser-Doppler anemometry to two-phase bubbly flows. A summary of available LDA-measurements in particulate, droplet and bubble flow systems is given which shows detailed measurements of signal properties and their dependence on optical parameters were not previously available. However, such information is necessary for optimizing the optical and electronic schemes for size measurements. Consequently, the signal characteristics of light scattered from single bubbles rising in quiescent water were obtained for a forward-scatter arrangement and for three different beam-intersection angles. In addition to the dependence of the signal properties of the bubble path through the beam-intersection region, the effects of aperture diameter and aperture position in the optical system are discussed. The resultant data were used to determine an optimum forward-scatter LDA-system which was then employed to measure the dependence of bubble velocity on bubble diameter over the range 0.2–1.0 mm. Finally, a theoretical model proposed to describe the dependence of the signal properties on the location of the centreline bubble path through the beam-intersection region is shown to be in agreement with the measurements. The treble amplitude peaks observed in the signals from bubbles in this size range are readily explained by applying the laws of geometrical optics.

1. INTRODUCTION

In research laboratories and university institutes all over the world, extensive studies are presently being conducted towards a better understanding of the fundamental mechanisms involved in transfer processes in two-phase flows. Besides theoretical interest, which aims at a deeper understanding of interphase momentum, heat and mass transfer, there is a strong demand for practical information to optimize those systems in which two-phase flows occur. Some of the current research activities are related to particulate two-phase flows with emphasis on experimental flow studies which provide a deeper understanding of the interactions between particles and the surrounding turbulent fluid flow. It is only recently that detailed studies of such flows have become feasible through the advent of laser-Doppler anemometry and its extension to flow systems with large particles.

Durst & Zaré (1975) and Durst (1978) developed the major ideas to carry out LDA-velocity measurements in flows containing large particles. It was claimed in previous studies that the light scattered by particles larger than the distance between the fringes, postulated to exist inside the measuring control volume, would produce signals with negligible modulation and hence, poor signal-to-noise ratio. However, Durst & Zaré (1975) and Durst (1978) showed that large particles can produce signals of excellent quality from which information on the particle velocity, particle size and particle concentration can be deduced. It was shown for single spheres that the signal is created from a fringe pattern in space produced by two reflected or refracted light beams. The fringe pattern is of complex shape and changes its position in space as the particle moves. It was also shown, the resulting signal frequency is independent of the detector location and is a function of the particle velocity. The shape and size of the fringe pattern permits information on the particle size to be deduced. Hence, extended LDA-systems can provide useful information on the fluid velocity via small particles in the flow and on the size and velocity of large suspended spherical particles. Information of this kind is needed in many areas in which particulate two-phase flows occur.

The aforementioned studies provided the basis for a number of successful measurements in two-phase flows and also gave explanations for previously observed phenomena. This is outlined in section 2 where a detailed literature survey is provided that shows the feasibility of two-phase flow velocity measurements using laser-Doppler techniques. This technique is now

well established and a number of measurements have been reported for flows with solid particles, droplets and bubbles. However, no detailed study has so far been reported on the LDA-signal characteristics and their dependence on the optical parameters. The present paper attempts to partially remedy this situation by providing information on the dependence of the LDA-signals on the location of the photodetector, the detector aperture, the position of the bubble inside the effective measuring control volume, etc. These dependences of LDA-signal properties need to be clearly understood to separate them from those that depend on the size and velocity of the bubble or particle to be studied.

Signal characteristics were recorded for air bubbles of controlled size and velocity rising in quiescent water. The optical arrangement described was applied to study the effects of variations in the location of optical components. Detailed results are presented for measurements carried out for three different beam intersection angles and for a detector location in the forward direction. The signal from the photomultiplier was digitized by means of a transient recorder and the signal frequency, pedestal amplitude and signal modulation depth (visibility) were determined by means of a mini-computer. The experimental equipment, the signal processing and the results are described in section 4. Results obtained with this equipment confirm the theoretical considerations given in section 3.

An optimized optical system was set up to measure the velocity of rising bubbles and to measure their size. Velocity data as a function of size are presented and it is shown that the present measurements agree well with previous data. In addition, the velocity of bubbles of given diameters were measured as a function of the distance from the tip of the generating nozzle.

2. LASER-DOPPLER MEASUREMENTS IN TWO-PHASE FLOWS: A BRIEF LITERATURE SURVEY

First attempts to carry out laser-Doppler measurements in particulate two-phase flows were undertaken by Lading (1971) and Davies (1973) in bubble flows. Davies (1973) showed the bubble velocity can be determined independently of the water velocity if the bubble size exceeds the size of the natural contaminants in the water. This finding was confirmed by Ohba (1977) who also used a reference-beam Doppler system to obtain local velocity information. Doppler signals from natural contaminants were employed to obtain local information on the water velocity from a photodetector located on the axis of the reference beam. Bubble information was recorded from a second detector off the axis of the reference beams. Davies (1973) showed the signal off the axis of the reference-beam exhibited good signal-to-noise ratios and remarkable modulation depth in spite of their large size.

LDA-measurements with dual-beam anemometers have also been undertaken and results have become available in particulate gas–solid phase flows, e.g. Farmer (1978), Riethmüller (1973), Carlson & Paskin (1975), Popper *et al.* (1975), Rolanski (1975), Stümke & Umhauer (1978). Farmer (1978) and Stümke & Umhauer (1978) studied the shape, amplitude and modulation depth of Doppler-bursts as a function of particle size using glass spheres up to several hundred microns in diameter. They found, in this size region, the signal modulation depth was well described by the following expression for the fringe visibility:

$$V = \frac{2J_1\left(\frac{\pi d}{2d_f}\right)}{\left(\frac{\pi d}{2d_f}\right)} \qquad [1]$$

where J_1 is the first order Bessel function.

Stümke & Umhauer (1978) found the particle material has an influence on the detected modulation depth, whereas, Farmer (1978) did not report this dependence in his investigations.

The first in-depth study of laser-Doppler anemometry in particulate two-phase flows was reported by Durst & Zaré (1975) who demonstrated with reflecting and transparent spheres that LDA-signals obtained from large particles can be explained as being generated by a fringe pattern located in space. This fringe pattern is produced by the two laser-beams of an LDA-optics being reflected and/or refracted by the particle which yields fringes in space that can be of rather complex shape. The instantaneous location of the interference pattern is dependent on the arrangement of the incident laser beams, the shape of the particle and its location with respect to the crossing region of the two incident light-beams. Furthermore, the rate at which the fringes cross a detector in space is linearly related to an effective velocity which is close to the transverse velocity component of the reflecting or refracting body, perpendicular to the axis between the two incident beams. In the backward direction, a linear fringe pattern is obtained with the fringe spacing observed at the detector being determined by the wave length of the laser light and the angle, β, formed by the detector position relative to the two reflecting points on the particle surface:

$$d_f = \frac{\lambda}{2 \sin \beta}. \qquad [2]$$

The small angle β is a function of the incident beam angle, the particle diameter and the position of particle trajectory through the laser beams. The frequency or rate at which the fringes cross any point in space is the same at all points and is equal to the rate at which fringes originate along a source line and disappear along a sink line. The Doppler frequency resulting from the movement of a non-deforming reflecting sphere is then:

$$f_D = \frac{2(U_\perp \cos \beta \pm U_\parallel \sin \beta) \sin \theta}{\lambda}. \qquad [3]$$

A similar equation was also given for transparent spheres and it was experimentally verified that this equation and the equation for reflecting particles correctly describe the measured Doppler frequencies.

Following up the work by Durst & Zaré (1975), a number of detailed measurements of particulate flows became available. Durst (1979) and Lee & Durst (1980) provided detailed particle velocity measurements in a turbulent pipe flow with suspended solid particles. For each test run, a constant particle size was chosen and experimental results were presented for different sizes. The results revealed the expected differences between the average fluid velocity and the local particle velocity and also showed the increase in turbulence intensities in the air flow expected for the investigated particle size range. They also found a particle free region for large particles in the vicinity of the pipe wall. This finding supported conclusions from their theoretical studies.

Measurements of the velocity of larger particles and their size have also been reported by Ungut *et al.* (1977, 1978) who applied a laser-Doppler anemometer for particle-velocity and particle-size measurements in combustion systems. Their verification experiments for the optical set-up were mainly carried out on solid particles that were moved through the measuring control volume in a well controlled way. Their final system was applied to liquid droplets in air and combustible gas mixtures. Solid particles in water flows were studied by Lee & Srinivasin (1978) with a reference beam system. The authors showed in their experiments that velocity information and particle size could be deduced from the optical signals they obtained.

Although the feasibililty of two-phase flow velocity measurements with laser-Doppler anemometry is now well established and several experimental results in simple boundary-layer flows and in separated flows with suspended particles have become available, information is still lacking on the influence of optical components on the characteristics of LDA-signals. The

study by Durst & Zaré (1975) did not consider the change of signal characteristics due to variations of the particle location with respect to the crossing region of the two light beams and the photodetector pinhole. The influence of the detector location and the size of the light collecting aperture have also not been investigated, although the explanations by Durst & Zaré (1975) suggest the influences exist. Without detailed knowledge of these influences, the interpretations of the signal characteristics in terms of particle velocity and particle size become difficult.

3. LASER-DOPPLER SIGNALS IN PARTICULATE TWO-PHASE FLOWS

3.1 *Signal-frequency and velocity information*

In a dual-beam laser-Doppler configuration, two equal strength laser-beams are focussed and crossed in a flow to form the measuring volume of the system, e.g. see Durst *et al.* (1976). A small particle of diameter, d, usually less than one fringe spacing, d_f, scatters light while passing through the fringe pattern postulated to exist in the crossing region of the two beams and the resultant signal from a photodetector shows an intensity variation due to the light intensity variations the particle experiences in the measuring control volume. The frequency of the photomultiplier signal, f_D, the particle velocity component, $U_\perp$, and the fringe spacing, d_f, are related by the following relationship:

$$f_D = \frac{U_\perp}{d_f} = \frac{2U_\perp \sin\theta}{\lambda}. \qquad [4]$$

By using this relationship, the velocity of the fluid phase can be determined in two-phase flows from the Doppler frequency of the signal generated by small particles present in the fluid (see Obha 1979).

To obtain velocity information for particles larger than the fringe spacing or even larger than the measuring control volume, information on the Doppler frequency is extracted from signals generated by reflected and/or refracted light beams (e.g. see Durst & Zaré 1975 and Durst 1978). Hence, for large particles signals of good signal-to-noise ratio can result from a fringe pattern being produced in space. Any motion of the particle from which the incident light beams are reflected or refracted causes the fringes to change their position. The resultant signal frequency from a stationary photodetector in space is again related to the particle velocity and the fringe distance in space by relationships which are similar to the one above and are given by Durst & Zaré (1975) and Durst (1978).

3.2 *Signal amplitude characteristics*

Total reflection of light occurs if a light-beam intersects the bubble surface at an angle normal to the surface larger than the critical angle,

$$\theta_c = \arcsin(1/n_W) = 48.75°. \qquad [6]$$

The light is only partially reflected and partially refracted if the incident angle with the normal to the surface is less than the critical angle. As a consequence of this fact, the two beams on an LDA-system incident on a bubble surface interfere beyond the bubble in space such that the Doppler bursts recorded in the forward direction exhibit three amplitude peaks with sinusoidal oscillations in each part of the signal, as shown in figure 1. Simple geometric optics can be used to explain the occurrence of the forward scatter triple-peaked laser-Doppler signals. The two side peaks are a result of the interference fringe pattern in space produced during the period of total reflection of the incident beam at the front and rear of the moving bubble as shown in figures 2(a) and 2(c). The central peak of the signal is a result of the interference of the partially refracted light beams that pass through the bubble as shown in figure 2(b) and interfere to

produce the central peak of the signal burst. As a bubble moves through the measuring control volume of a LDA-system, the fringe pattern indicated in figures 2(a)–2(c) will subsequently pass a photodetector located in the forward direction and yield triple-peaked laser-Doppler signals as shown in figure 1.

The existence of LDA-signals from large particles that exhibit three amplitude peaks has not been documented before, although, Wigley (1978) correctly explained their existence. In his experiments, he only demonstrated double-peak signals in the forward direction due to the reflection from metal wires. Wigley (1978) observed, however, a single-peaked signal in the backward direction. Its existence can be readily deduced from figure 3(b). Figures 3(a) and 3(c) explain the double peaked signal observed by Wigley in the forward direction.

The aforementioned considerations suggest, in agreement with Durst & Zaré (1975) and Durst (1978), the existence of fringe patterns in space that move as the originating bubble or particle moves and yield the resultant Doppler signals if the detection system is designed to spatially resolve the fringes. For detection systems with finite apertures, integration over several fringes will occur if the aperture exceeds the fringe spacing. This yields detected signals with properties that can be computed by integrating the light-intensity distributions in space over the area of the finite aperture. Considering the special bubble location in figure 4, and the coordinate system (u, v, w) given in the same figure, the light-intensity distribution at the detector aperture can be written as follows:

$$I^* = \frac{1}{2\cos\alpha}\exp\left[-\frac{2}{b_0^2}(u^2 + v^2\cos^2\alpha + w^2\sin^2\alpha)\right] \times \left[\cos^2\alpha\left[\cosh\left(\frac{2vw\sin\alpha/2}{b_0^2}\right) + \cos\left(\frac{2\pi v}{d_f}\right)\right]^2 + \sin^2\alpha\sinh^2\left(\frac{2vw\sin\alpha/2}{b_0^2}\right)\right]^{1/2}. \quad [8]$$

The above equation only correctly applies at a distance equivalent to the distance where the centre of the two refracted wave fronts cross. The aperture of the detection system is assumed to be located at this crossing point. Due to its finite size aperture, the detection system will yield an output signal proportional to the integral light power penetrating the aperture surface at an instant in time. Hence, the resultant signal is proportional to the light power computed as follows:

$$P_s^* = \frac{1}{2\left|\frac{\pi a^2}{4}\right|\cos\alpha}\int_{-(a/2)}^{+(a/2)}\int_{-\sqrt{(a/4)^2-v^2}}^{+\sqrt{(a/4)^2-v^2}}\left\{\exp\left[-\frac{2}{b_0^2}(u^2 + v^2\cos^2\alpha + w^2\sin^2\alpha)\right] \times \left[\cos^2\alpha\left[\cosh\left(\frac{2vw\sin\alpha/2}{b_0^2}\right) + \cos\left(\frac{2\pi v}{d_f}\right)\right]^2 + \sin^2\alpha\sinh^2\left(\frac{2vw\sin\alpha/2}{b_0^2}\right)\right]^{1/2}\right\} du\,dv$$

where a is the diameter of the detector aperture.

Numerical integration of this equation yields the final results that can be presented as a function of the ratio of aperture diameter, a, to fringe spacing,† d_f. Computations of signal visibility (modulation depth), the amplitude of the signal pedestal and the amplitude of the Doppler signal are given in figures 5(a)–5(c).

†The fringe spacing has to be taken at the location of the detector aperture.

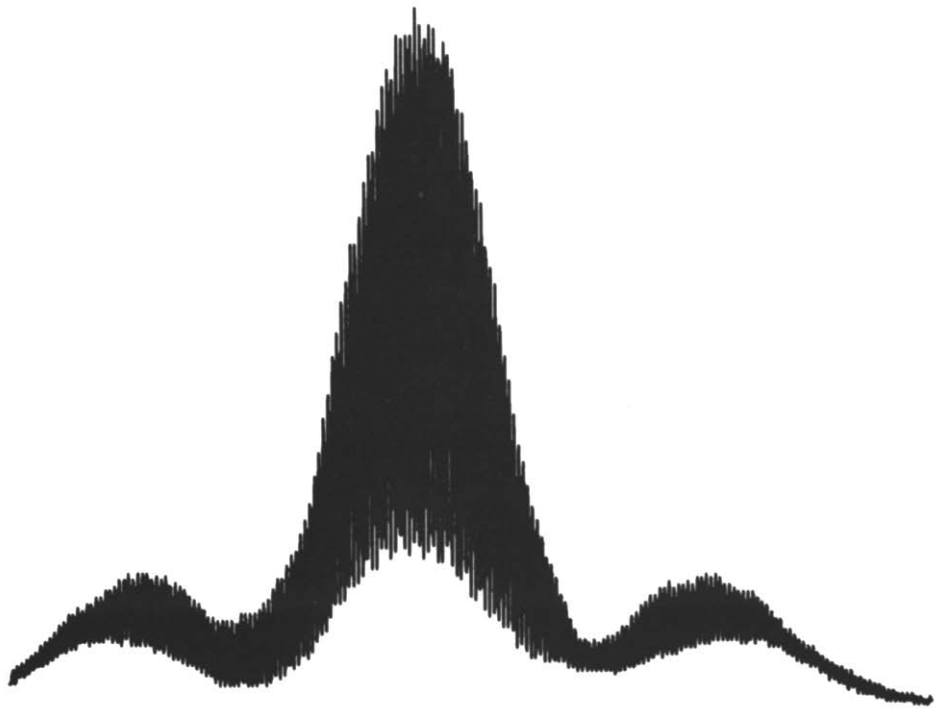

Figure 1. Typical Doppler burst recorded in forward scatter.

Equation[8] also permits the dependence of the Doppler signal properties on trajectory position of the bubble through the measuring volume to be computed. A small displacement of the bubble trajectory off the axis of the optical system and perpendicular to the plane of the two laser beams results in a shift in the position of the centre of the fringe pattern from the centre of the detector as shown in figure 6. It can be shown by geometric optics that this displacement of the bubble results in a shift in the u-position of the fringe pattern relative to the collecting aperture. For large values of the ratio of detector distance and bubble diameter, i.e. $L/d \geqq 10$, the shift is given by the following relationship:

$$u = 0.66\left(\frac{L}{r}\right) \cdot x. \qquad [10]$$

Figure 7 shows the results of the numerical integration of the fringe pattern over the detector aperture for various u-positions. A similar integration can also be applied to the z-trajectory displacement of the bubble. The theoretical results for a single bubble diameter show the visibility is independent of the bubble x-trajectory position, at least over a finite central position of the measuring volume and, therefore, can be used to uniquely correlate signal visibility to bubble size. The Doppler and pedestal amplitudes are not constant with respect to the x- and z-trajectories of the bubble. Consequently, an appropriate trajectory discrimination routine is required if bubble size is to be correlated with either the Doppler or pedestal amplitudes.

4. EXPERIMENTAL INVESTIGATIONS

4.1 *Experimental equipment and data recording*

The present experiments were performed to verify the theoretically predicted influences of system components and their relative locations on characteristics of LDA-signals obtained from large bubbles. To carry out quantitative experimental studies, a 5-mW He–Ne laser was used in a dual-beam laser-Doppler anemometer configuration. The forward optics was of modular design consisting of a beam splitter, a neutral density filter, mounting hardware and three

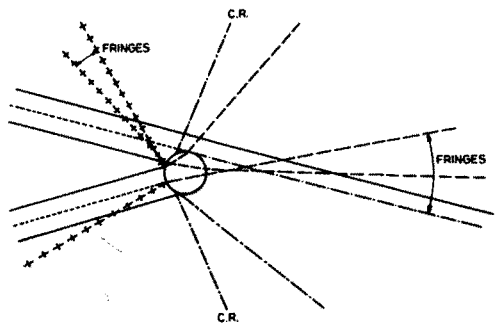

Figure 2(a).

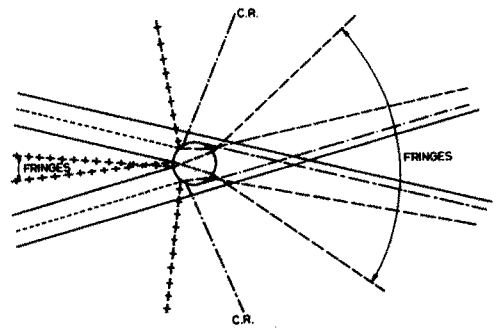

Figure 2(b).

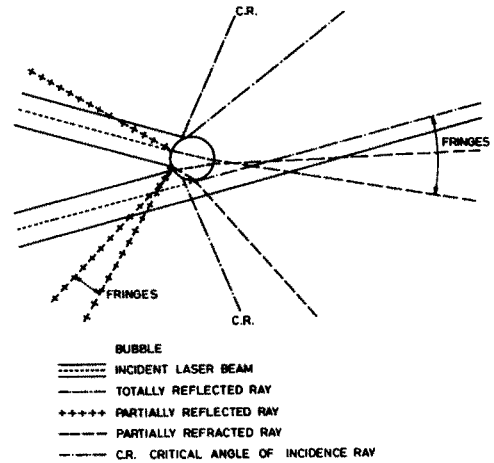

Figure 2(c).

Figure 2. Sketch to explain triple peaked Doppler burst of a bubble.

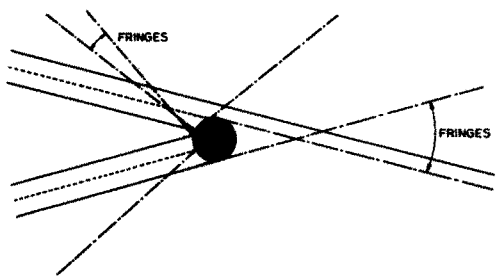

Figure 3(a).

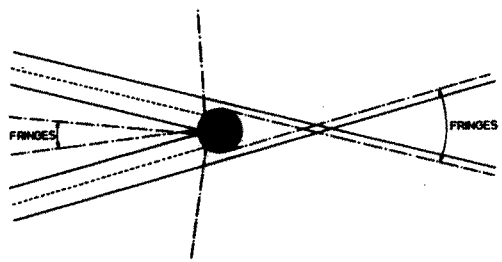

Figure 3(b).

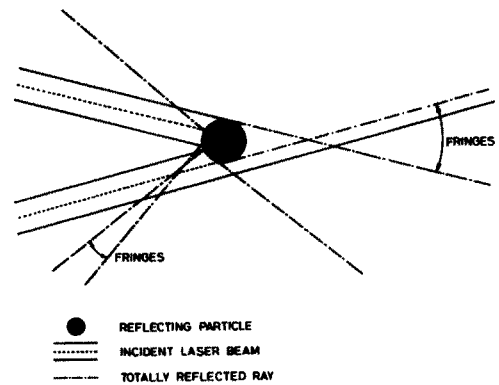

Figure 3(c).

Figure 3. Sketch to explain double peaked Doppler burst as recorded by Wigley (1978).

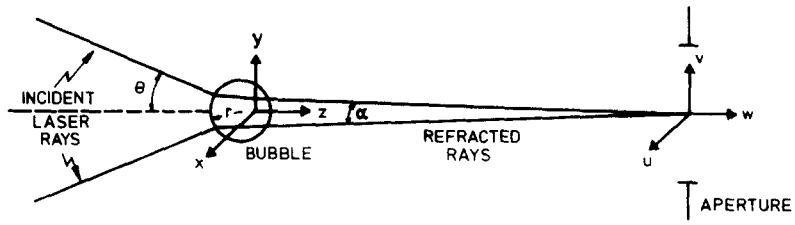

Figure 4. Interference of light in forward direction and coordinate system.

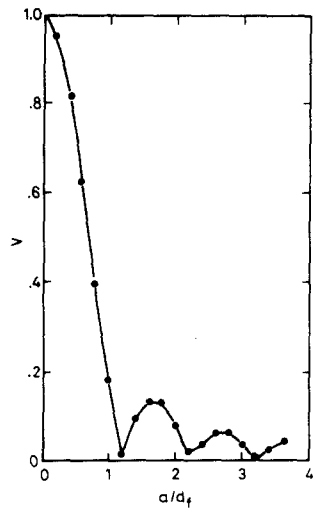

Figure 5(a).

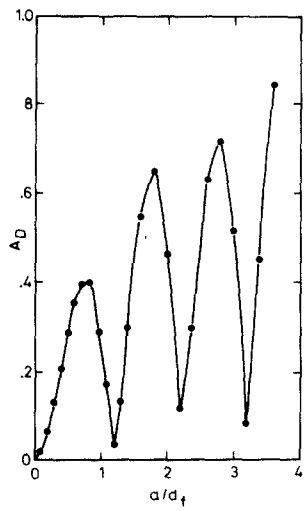

Figure 5(b).

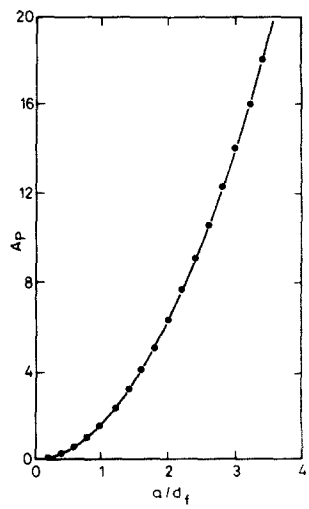

Figure 5(c).

Figure 5. Computed amplitude characteristics of finite aperture averaged intensity distribution.

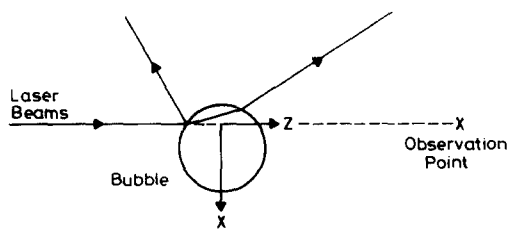

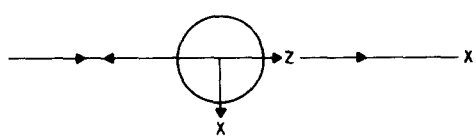

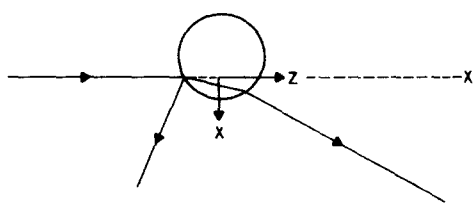

Figure 6. Displacement of fringe pattern due to shift of bubble location in the x-direction.

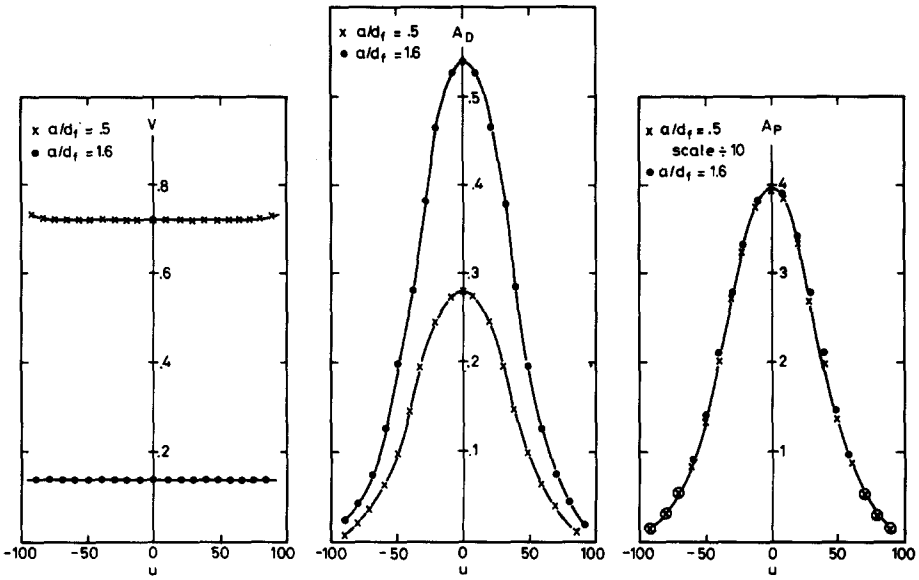

Figure 7. Computed amplitude characteristics of finite aperture averaged intensity distribution for shift of bubble location in the x-direction.

interchangeable lenses of 120, 250 and 600 mm focal lengths. The collecting optics consisted of a 150-mm focal length lens and a translating photomultiplier assembly mounted on a leveling base (see figure 8a). The photomultiplier housing and the 0.3-mm-dia. pinhole on the front were both movable in two dimensions. A variable-diameter "metal leaf" aperture, suspended from above on a two-dimensional translation mechanism, was positioned on the centre line of the receiving optics and 43 mm behind the light collecting lens. The diameter of the aperture was variable from 2 to 32 mm. Translation was possible in the vertical and horizontal planes with displacement scales calibrated in 0.025-mm intervals.

The laser-Doppler optics were placed on tables positioned in a "T" pattern with the flow channel in the centre as shown in figure 8(a). Two laser beams were focused in a vertical plane to a point in the vicinity of the centre of a flow channel. The intersection region of the beams was set approx. 30 mm above the position of bubble formation. Forward and 90° scatter experiments were performed and in each case with the centreline of the collecting lens positioned approx. 320 mm away from the intersection region of the laser beams. In this paper, details of the experiments and results are only provided for the forward scatter experiments.

Compressed air was passed through a small glass nozzle to generate bubbles at a constant rate. The bubbles rose through still water in a square plexiglass container of 25.4 mm i.d. The size of the bubbles and their terminal velocities were controlled by regulating the air pressure between 68.9 and 206.8 kPa from a compressed air cylinder. The glass air nozzle was hand-made from a capillary tube (5.5 mm o.d., 0.75 mm i.d.) which was heated with an acetylene torch and stretched out very carefully to form a long tapered nozzle. The end was cut off under a microscope at the point where the inside wall of the capillary tube collapsed to solid glass giving an exit i.d. of 0.011 ± 0.005 mm. Since the alignment of the collection optics was critical, the water container was positioned on a horizontal two-dimensional translation table. Displacement of the table could be controlled to within 0.0125 mm allowing the bubble trajectory through the intersection region of the laser beams to be determined with an accuracy of 0.0125 mm sufficient for the present study.

A 16-mm Hycam movie camera was employed to photograph the bubbles as they rose through the water. Illumination for these photographs came from backlighting the water

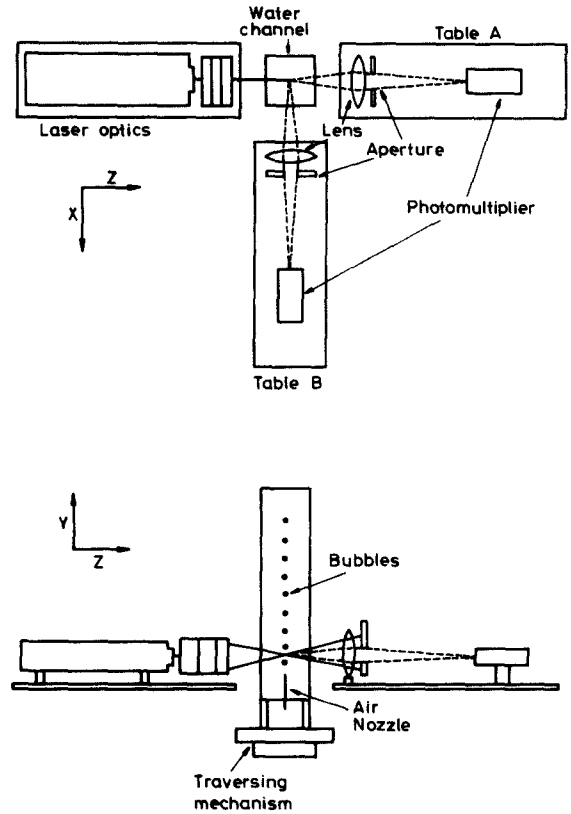

Figure 8(a). Optical arrangement, traversing arrangement and x-y-z coordinates.

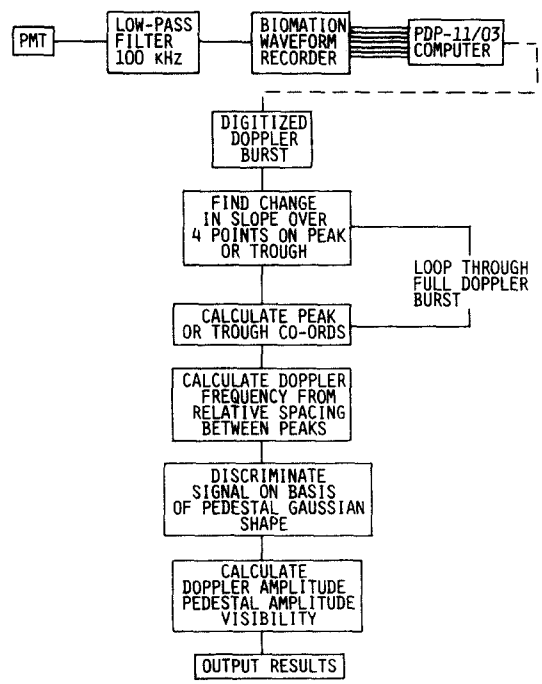

Figure 8(b). Block diagram of data recording and processing equipment; flow chart of software program.

channel through a thin tissue diffuser. A wire, 0.508 mm in diameter, suspended down the centre of the channel established a reference dimension from which the diameter of each bubble in the picture could be determined. Kodak 16 mm 4-X Reversal 7277 film was found to work well under the restricted light conditions since it offered good speed and acceptable grain size upon enlargement. The bubble diameter was measured with a photo-optical data analyzer consisting of a flicker free, multiple speed projector and viewing screen with a positional transducer based X-Y-pointer mechanism linked to a microprocessor. The microprocessor offered fully programmable scale and reference zero-point definition and digitally output X and Y coordinates to a line printer.

A Biomation, model 8100, 8-bit transient recorder was used to digitize the photomultiplier output signals. It incorporates a 100-MHz, analog-to-digital converter integrally connected with a 2048 word memory. A Digital Equipment Corp. PDP-11/03, computer system was interfaced to the Biomation transient recorder allowing real time analysis of all Doppler bursts.

Doppler signals from the photomultiplier were low-pass filtered at 100 kHz to remove some of the inherent high frequency shot noise and then digitized by the Biomation transient recorder at a 0.5 MHz–2 MHz rate depending on the Doppler frequency. Triggering of the Biomation unit was set to collect a full Doppler burst in at least 1024 points of the memory. Software programs were used for on-line analysis of the Doppler burst frequency, signal visibility (modulation depth), Doppler amplitude, and pedestal amplitude. Only "amplitude discriminated" bursts were recorded so that only "good" Doppler bursts of sufficient amplitude and yielding correct Doppler information were processed.

The amplitude characteristics were computed as functions of the collection cone angle, its magnitude and direction relative to centreline and the position of bubble trajectory through the intersection region of the laser beams for a constant bubble diameter of 0.57 mm. Three different laser beam intersection angles in water, namely 9.51, 4.35 and 1.84° were used in each experiment.

A change in the diameter of the aperture of the collection optics results in a change in the magnitude of the collection cone angle and the intensity of scattered light focused on the photomultiplier. To study this influence on the signal properties, the aperture diameter was increased, 1 mm at a time from its minimum diameter of 2 mm. The directional dependence of the collection cone angle was investigated by moving the aperture relative to the axis of the collecting optics. Increments of 1 mm were used in moving the 2 mm diameter aperture in the horizontal and vertical directions of a plane parallel to the collecting lens plane. The trajectory dependence of the bubble was studied by positioning the water container such that the bubble trajectory passed through equally spaced intervals along the major and minor axis of the plane of the elliptical probe volume.

The optimum dual-beam laser-Doppler configuration suggested by these experiments was used to study the effect of bubble size on the amplitude characteristics of Doppler bursts. A visibility of approx. 0.5 for a bubble diameter in the middle of the air nozzle's dynamic range of sizes was used as the criteria for choosing the best configuration. This was employed to obtain the velocity and size measurements of rising bubbles described in section 5.

4.2 *Signal processing*

Signal processing was performed by the electronic system and software indicated in figure 8(b). Doppler frequency and amplitude characteristics were determined by calculating the relative position and amplitude of each peak and trough in the digitized sinusoidal signal over the entire burst. The points before the actual midpoint of a peak or trough were found by detecting a change in slope over four consecutive points. An interpolation routine was used to calculate the time-amplitude co-ordinates of the peak and trough midpoints using these four

surrounding points. The Doppler frequency was calculated by determining the relative time spacing between consecutive peak midpoints and averaging over a number (20 and more) of the intervals symmetric around the maximum amplitude in the burst profile.

The Doppler amplitude, pedestal amplitude and visibility were calculated in two ways. In one case, the largest amplitude peak and next consecutive trough in the Doppler burst were used. In the other, the amplitude of three peaks, one either side of the largest peak, and their corresponding troughs were averaged to define a mean peak and a mean trough amplitude. These were employed to calculate the mean Doppler amplitude, pedestal amplitude and visibility. The second method was found to be a more reliable estimate of the amplitude characteristics because it averaged out minor noise fluctuations and small inaccuracies in the interpolation routine.

Two discrimination routines were incorporated into the soft-ware to distinguish "good quality" Doppler bursts. The incorporated frequency discrimination was based on the S.D. in the magnitude of the time separation between peaks in Doppler bursts. If the deviation due to noise or a non-specific shift in frequency was greater than a specified value set to be 2 per cent, the Doppler burst was rejected. A Gaussian-shape discrimation routine was employed to eliminate Doppler signals which did not exhibit Gaussian pedestal profiles. The calculated peak and trough points were used to define a set of points representing the pedestal profile. A Gaussian transformation was applied to the pedestal points and a linear correlation cofficient of 1.0 indicated exact Gaussian pedestal behaviour.

4.3 *Results of signal characteristic measurements*

Considerations described in the sections up to section 3 revealed a dependence of characteristics of LDA-signals from large particles on size and velocity as well as the configuration of the optical components. In order to separate the latter from the former, experiments were performed with a single bubble size and rise velocity and the effects of the optical components on LDA-signal properties were quantified.

The data presented for Doppler frequency, Doppler amplitude, pedestal amplitude and visibility were computed from digitized bursts for which the correlation between the pedestal shape and a Gaussian curve was greater than 0.85. The sensitivity of the results to the averaging ensemble size for a given optical configuration and bubble size and trajectory through the measuring volume was obtained prior to the final measurements and it was found that reliable estimates of all the burst parameters could be obtained from ensemble averages with as few as 25 bursts by using this Gaussian pedestal discrimination. The laser-Doppler frequency was found to be constant within less than 1.5 per cent, when averaged over this number of bursts, even when the data from extreme opposite ends of the measuring volume were taken. This result indicated the angle variation due to different z-locations of the bubbles are negligible for most practical applications.

All Doppler bursts recorded in the forward scatter direction exhibited the three peaks in the signal shape shown in figure 1 and discussed in section 3. In order to compute the amplitude dependence of LDA-signals on parameters of the optical system, only the center signal peak was taken into account.

The amplitude characteristics of Doppler bursts in forward scatter as a function of the limiting aperture diameter and the beam intersection angle are presented in figures 9(a)–9(c). The visibility of Doppler bursts is shown to decrease with an increase in the beam intersection angle and an increase in the aperture diameter. This behaviour is predominantly due to the dependence of the pedestal amplitude on these parameters.

In the forward scatter direction, a larger modulation depth of the signals is observed with smaller beam intersection angles as shown in figure 10(a), where the signals obtained for a 4-mm

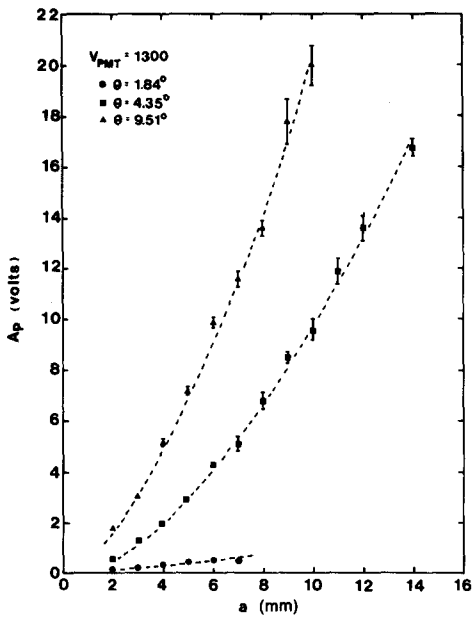

Figure 9(a).

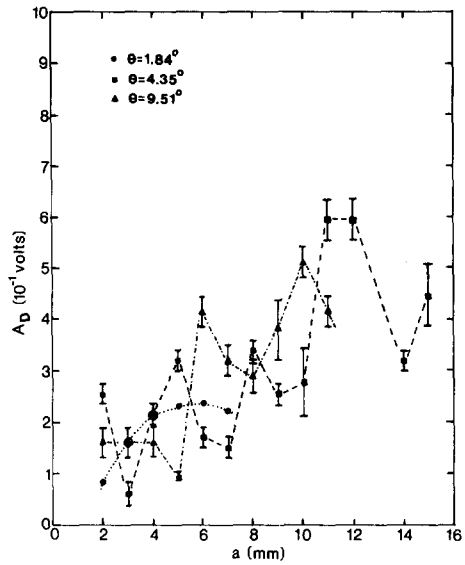

Figure 9(b).

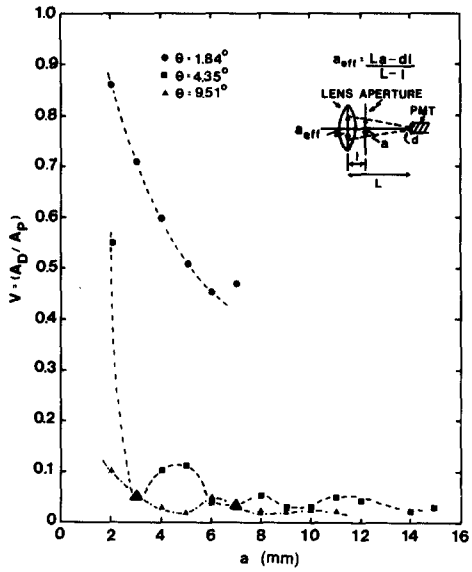

Figure 9(c).

Figure 9. (a) Pedestal amplitude as a function of aperture diameter for a bubble of diameter $d = 0.57$ mm. (b) Doppler amplitude as a function of aperture diameter for a bubble of diameter $d = 0.57$ mm. (c) Visibility as a function of aperture diameter for a bubble of diameter $d = 0.57$ mm.

dia. aperture and three intersection angles are compared. An increase in the relative amplitude between the side peaks and the central peak of the Doppler bursts can be seen for decreasing beam intersection angles such that the side peak amplitudes are almost equal to the central peak amplitudes for $\theta = 1.84°$. For large aperture diameters, in excess of 6 mm for $\theta = 1.84°$, the side peaks influence the shape of the central peak distorting the Gaussian pedestal (see figure 10b). Further increases in the aperture diameter reduce the modulation depth (visibility) of the signal.

As theoretically shown in section 3, the amplitude characteristics of Doppler-bursts depend on the position of the bubble trajectory in the x–z-plane. The effects of shifting the bubbles'

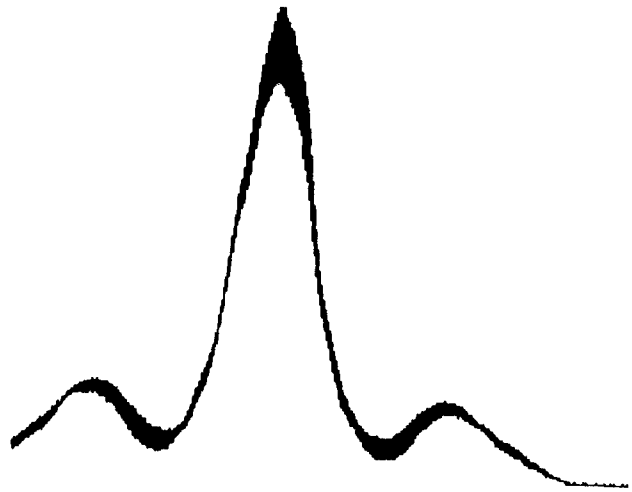

(i)

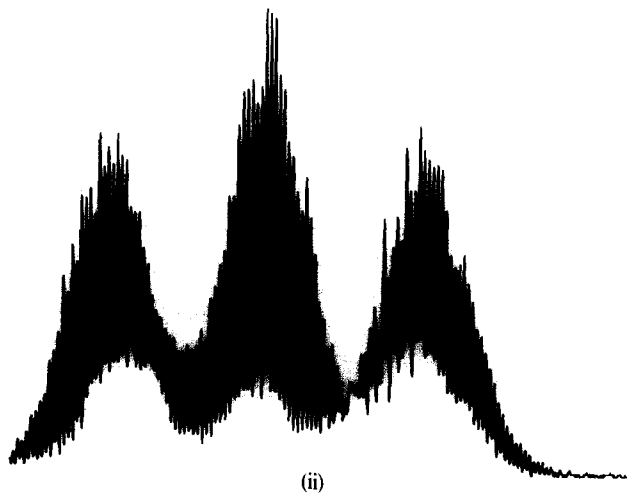

(ii)

Figure 10(a). Comparison of forward scatter Doppler bursts, $d = 0.57$ mm, $a = 4$ mm, (i) $\theta = 4.35°$, (ii) $\theta = 1.84°$.

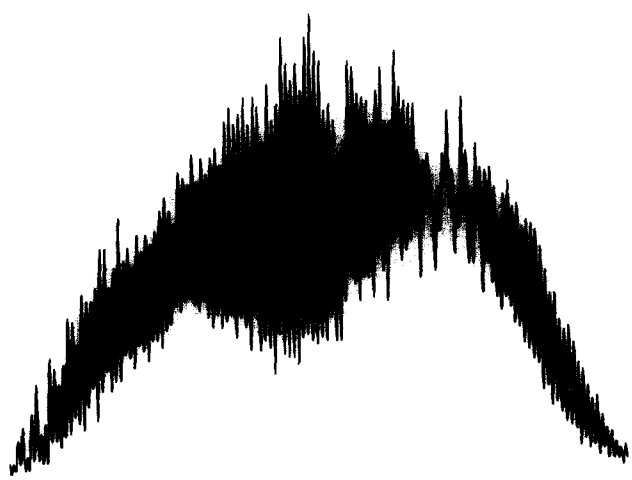

(i)

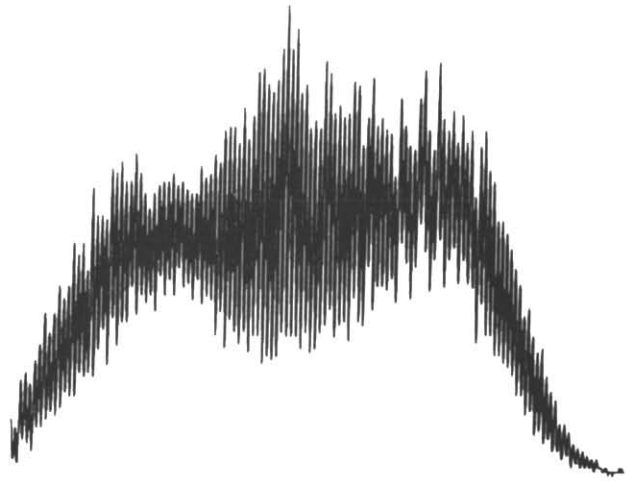

(ii).

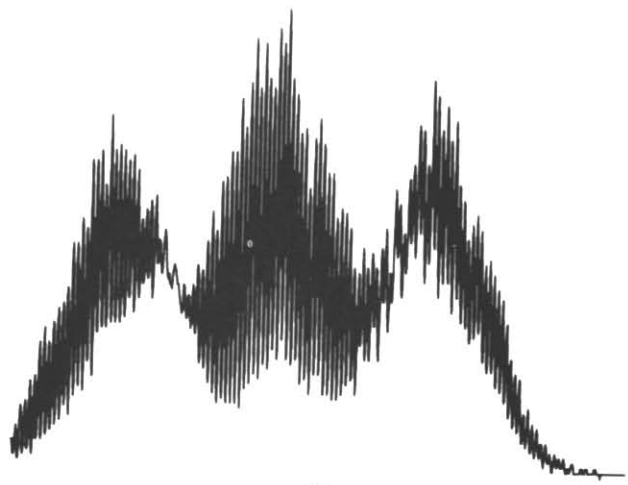

(iii)

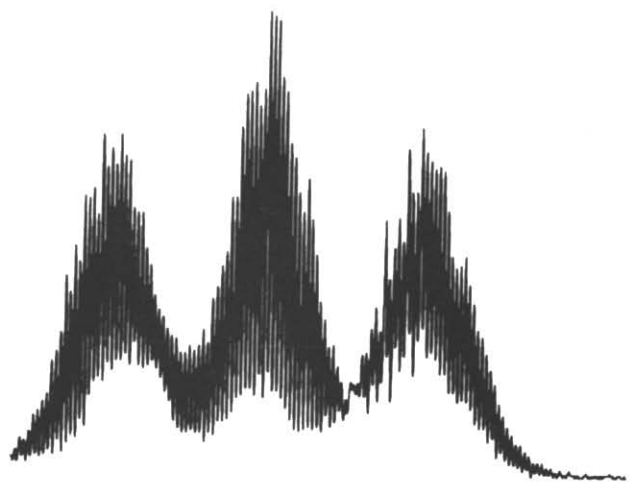

(iv)

Figure 10(b). Distortion of central peak profile by side peaks as a function of aperture diameter $\theta = 1.84°$ $d = 0.57$ mm.

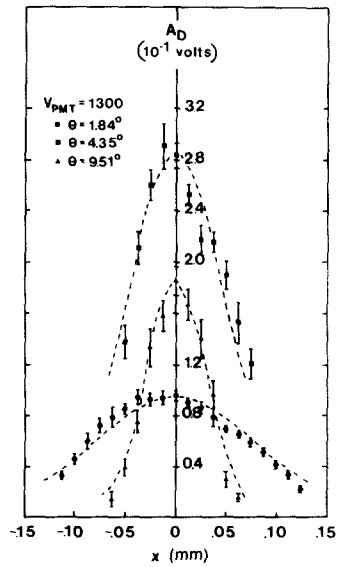

Figure 11(a).

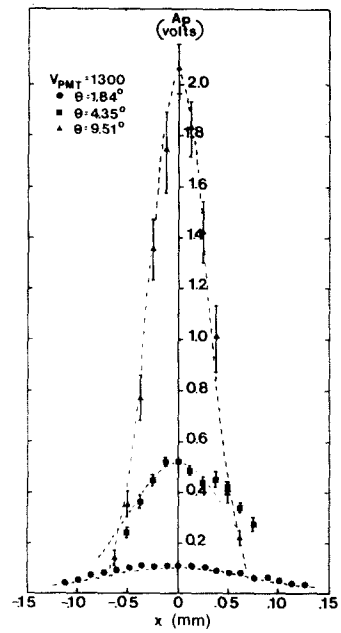

Figure 11(b).

Figure 11. (a) Doppler amplitude as a function of bubble x-position of trajectory $a = 2$ mm $d = 0.57$ mm. (b) Pedestal amplitude as a function of bubble x-position of trajectory $a = 2$ mm $d = 0.57$ mm.

x-position, with the z-position set for maximum amplitude in forward scatter, are presented in figures 11(a) and 11(b). The Doppler amplitude variation is, for all angles between the incident light beams, well represented by Gaussian profiles. Pedestal amplitude variations show the same Gaussian trends. Table 1 summarizes the amplitude parameters which can be used to define the spatial extent in the x-direction over which good quality bursts can be obtained. The data show the Doppler and pedestal e^{-1}-amplitude widths are equal. They are, however, an order of magnitude smaller than the e^{-1}-intensity width of the probe volume. Constant visibility is observed in the data for all three beam intersection angles over the range in which good quality bursts are observed as implied by the corresponding data in figures 11(a) and 11(b).

Table 1. x-Direction amplitude resolution characteristics

Beam Inter-section angle θ	Scatter direction	Doppler amplitude e^{-1} width	Pedestal amplitude e^{-1} width	Per cent difference	Probe Volume e^{-1} intensity width
1.84°	Forward	0.118 mm	0.118 mm	0	1.05 mm
	90°	—	—	—	
4.35°	Forward	0.073 mm	0.070 mm	4.2	0.44 mm
	90°	0.088 mm	0.093 mm	5.5	
9.51°	Forward	0.045 mm	0.040 mm	11.8	0.20 mm
	90°	0.045 mm	0.043 mm	4.5	

The effect of shifting the bubbles' z-position with the x-position set for maximum amplitude in the forward scatter are presented in figures 12(a) and 12(b). The Doppler and pedestal amplitude data generally display linear behaviours rather than the distinct Gaussian behaviour exhibited for the shift in the x-direction. Table 2 compares the extent of the shift in the z-direction for (good quality Doppler bursts) to the probe-volume length. Again, the region over which good signal bursts can be obtained is smaller than the actual extension of the measuring volume. Similar to the data in figures 11(a) and 11(b), constant visibility was observed over the range of good Doppler bursts for each beam section angle.

Table 2. z-Direction "good quality" Doppler burst resolution

Beam intersection angle θ	Scatter direction	Resolution	Probe volume length 1 m
1.84°	Forward	4.0 mm	24.48 mm
	90°	—	
4.35°	Forward	0.64 mm	4.38 mm
	90°	0.23 mm	
9.51°	Forward	0.20 mm	0.91 mm
	90°	0.20 mm	

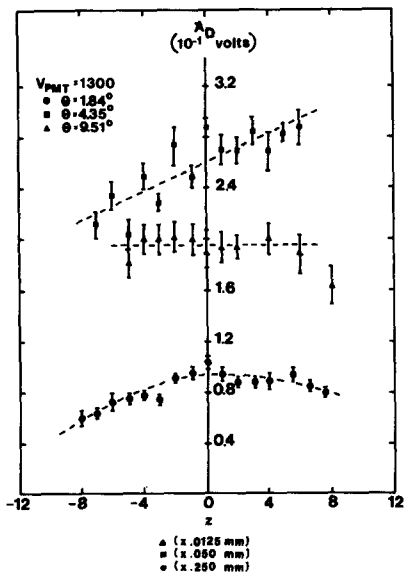

Figure 12(a).

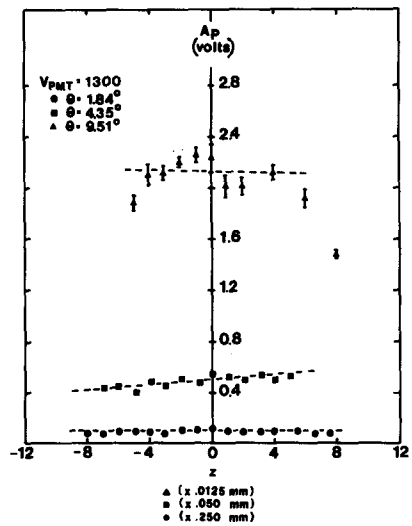

Figure 12(b).

Figure 12. (a) Doppler amplitude as a function of bubble z-position of trajectory $a = 2$ mm $d = 0.57$ mm. (b) Pedestal amplitude as a function of bubble z-position of trajectory $a = 2$ mm $d = 0.57$ mm.

Studies of the effects of the aperture location (off the axis of the optics) on the signal properties were also performed and suggest the centralized aperture to be optimum.

Measurements were also performed by the 90° scattering arrangement shown in figure 8(a). Similar conclusions can be drawn from these data (e.g. Liska 1979).

5. OPTIMIZED LDA-SYSTEM AND SIMULTANEOUS MEASUREMENTS OF BUBBLE SIZE AND RISE VELOCITY

The information provided in the previous chapters was employed by the authors to set up an optical system for local, simultaneous measurements of size and velocity of rising air bubbles in quiescent water. The optimum laser-Doppler configuration for bubble diameters up to 1.0 mm possessed a beam intersection angle of $2\theta = 8.7°$ measured in water and a 2-mm dia. limiting aperture centred along the axis of the collecting optics. A 3-mm dia. aperture was also incorporated for comparison and to increase the measuring accuracy for smaller bubble sizes. All other parts of the optical systems remained as described in section 4.1.

Prior to the final measurements, the LDA-signal characteristics were calibrated as a function of bubble size where the latter was taken from high speed photography records obtained simultaneously with the LDA-signal records. The resultant measurements of signal visibility, signal Doppler amplitude and signal pedestal amplitude are given in figures 13(a)–3(c) for both the 2- and 3-mm dia. apertures. The visibility monotonically decreases with increasing bubble diameter. The 3-mm aperture diameter data asymptotically approaches a minimum visibility of 0.075 beyond a bubble diameter of 0.8 mm. In contrast, the 2-mm aperture data allows

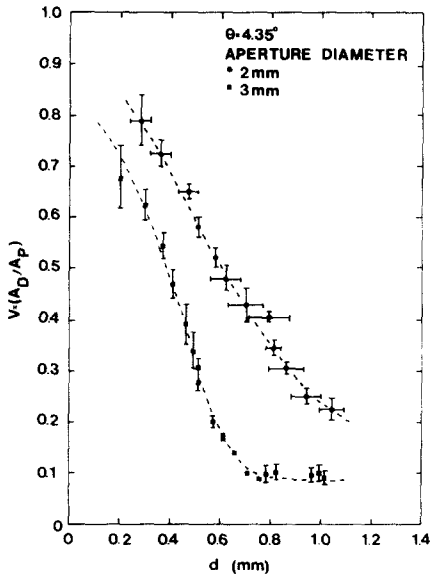

Figure 13(a).

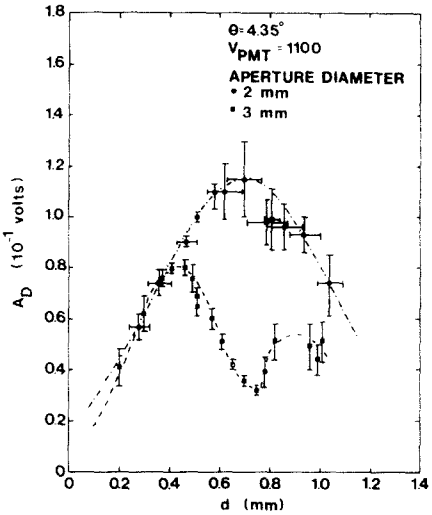

Figure 13(b).

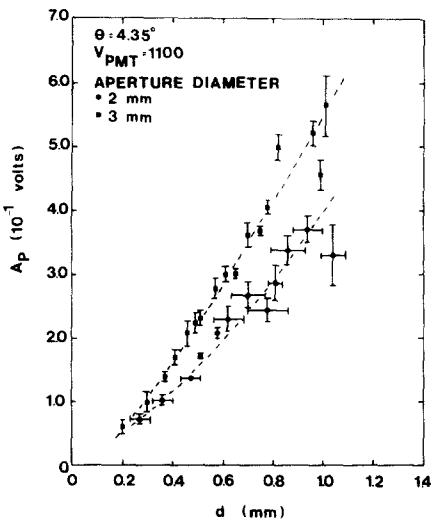

Figure 13(c).

Figure 13. (a) Visibility as a function of bubble diameter. (b) Doppler amplitude as a function of bubble diameter. (c) Pedestal amplitude as a function of bubble diameter.

measurements over a much larger range of bubble diameter. Consequently, the bubble diameter range for unambiguous correlation with visibility is increased with decreasing diameter of the limiting aperture in the light collecting system. The results also show the pedestal amplitude increases monotonically with increasing bubble diameter for the 2- and 3-mm dia. apertures. The larger the aperture diameter, the larger the pedestal amplitude for the same bubble diameter.

Utilizing the information in figures 13(a)–13(c) and the known relationship between the measured Doppler frequency and the bubble velocity, permitted the local size and velocity of rising air bubbles in water to be determined. The bubble velocity and signal visibility (as a measure of bubble size) were first recorded as a function of the translated height above the nozzle. Figure 14 shows a typical set of data which indicates the asymptotic velocity is reached at a height of 40 mm. This height was kept constant for all simultaneous measurements of

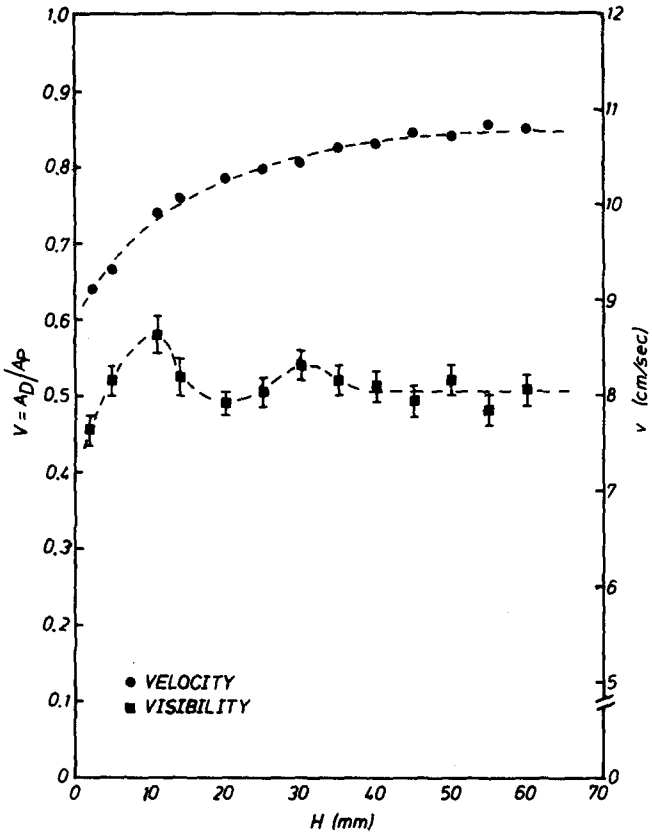

Figure 14. Bubble velocity and visibility (bubble diameter) as a function of distance from nozzle for single bubbles rising in water.

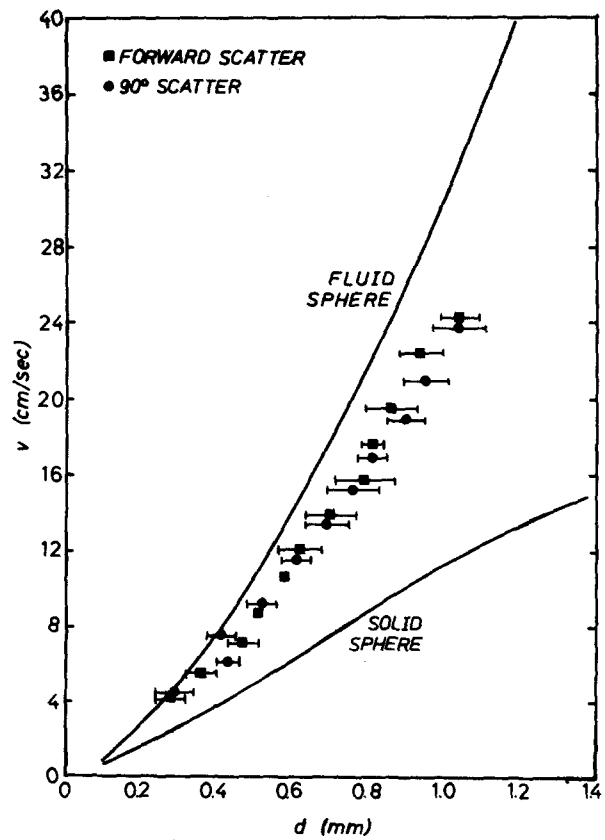

Figure 15. Correlation between bubble velocity and bubble diameter.

bubble rise velocity and bubble size. Results of these measurements are presented in figure 15. The data were corrected for wall effects by using the drag correction equation derived by Happel & Bart (1974) for spheres moving along the axis of the square water container. Previous empirical correlations for both fluid and solid sphere behaviour, outlined by Wallis (1974), are presented for comparison.

6. CONCLUSIONS AND FINAL REMARKS

The results of the present paper confirm the applicability of laser-Doppler systems to bubble velocity measurements to yield local information with high accuracy. Actual measurements were performed over the bubble diameter range $0.2\,\text{mm} \leqq d \leqq 1.0\,\text{mm}$. Various optical configurations were employed with fringe spacings several hundred times smaller than the bubble diameters. The resultant signals also permitted size information to be deduced. The investigations showed optimized LDA-systems yield no significant ambiguity due to bubble trajectory or variations in optical arrangement if the signal bursts used for measurements are discriminated on the basis of signal pedestal shapes, signal amplitude and signal quality.

The signals in the forward scatter direction show three amplitude peaks that have not been previously documented. The two side peaks on either side of the central peak are due to the period of total reflection which occurs as the bubble interface just enters and leaves the measuring volume as discussed in Durst (1978). Their presence requires caution be used in employing forward scatter signal characteristics for the purpose of measuring bubble size since the signal can be incorrectly interpreted as the result of three different bubbles traversing the measuring volume.

The extensive data on the amplitude characteristics for forward scatter signals show the visibility function is uniquely related to bubble size, independent of trajectory, over a range which depends on the aperture size of the light collecting optics. A unique correlation of the pedestal amplitude with bubble diameter is also possible if a further level of discrimination is employed to eliminate the dependence on the location of the trajectory in the measuring volume along the laser axis.

Finally, the behaviour of the signal visibility (modulation depth) as a function of aperture diameter for large bubbles is very similar to the LDA-signal dependence on particle size for particles two orders of magnitude smaller than the investigated bubbles, i.e. of the order of the fringe spacing (see Farmer 1978). A fringe model was proposed (see also Liska 1979), which describes the fringes that develop in space due to the interference of two beams reflected and/or refracted at the bubble interface. The model successfully predicts the qualitative signal-behaviours observed in the experiments for variations of aperture diameter of the receiving optics. It also successfully explains LDA-signal property variations caused by variations of the bubble trajectory across the measuring volume. A quantitative model requires a much more detailed analysis but this simple model supports the explanation of the signal formation mechanisms for two-phase flow put forward by Durst & Zaré (1975) and Durst (1978) and indicates a significant advancement in the present understanding of LDA-measurements in two-phase flows.

Although not discussed in the present paper, simultaneous measurements of the velocity of the liquid phase would be a straight forward extension of the LDA-system discussed here. Suitable optical configuration and electronic signal-processing systems to measure both phases have been given by Durst (1978).

Acknowledgements—The research described in this paper is the outcome of a cooperative program between the Sonderforschungsbereich 80 of the Universität Karlsruhe and the Department of Mechanical Engineering of the University of Toronto. The present work was carried out at Toronto and is based on the M.A.Sc. Thesis of J.J. Liska. Some data were also obtained by G. Chandler.

Financial support for the research work was obtained from NSERC Grants A9196 and A4172 and the Thomas Hogg Overseas Fellowship (for J. J. Liska), Valuable assistance in building electronic components was received from M. Kalovsky and D. Clayton assisted with the work during the high speed photography studies. The authors are also grateful to S. McKay for finalizing the figures and to A. Cowieson and G. Bartman for typing the manuscript.

REFERENCES

CARLSON, C. R. & PESKIN, R. L. 1975 One-dimensional particle velocity probability densities measured in turbulent gas-particle duct-flow. *Int. J. Multiphase Flow* **2**, 67–78.

DAVIES, W. E. R. 1973 Velocity measurements in bubbly two-phase flows using laser-Doppler anemometry. Institute for Aerospace Studies, University of Toronto, Part I and II, UITAS-Technical Notes 184–185.

DURST, F. 1978 Studies of particle motion by laser-Doppler techniques. *Proc. Dynamic Flow Conf.* 1978, Marseille and Baltimore, pp. 345–372, September.

DURST, F. 1979 Laser-Doppler Anemometrie und ihre Anwendung in Einphasen-und Zweiphasenströmungen. *PARTEC-Proc.* Nürnberg, pp. 361–390.

DURST, F., MELLING, A. &WHITELAW, J. H. 1976, *Principles and Practice of Laser-Doppler Anemometry.* Academic Press, New York.

DURST, F. & ZARÉ, M. 1975 Laser-Doppler measurements in two-phase flows. *Proc. LDA-Symp.* Copenhagen, pp. 403–429, August.

FARMER, W. M. 1978 Measurements of particle size and concentrations using LDV-techniques. *Proc. Dynamic Flow Conf.* 1978, Marseille and Baltimore, pp. 373–396, September.

HAPPEL, J. & BART, E., 1974 The settling of a sphere along the axis of a long square duct at low Reynolds numbers. *Appl. Scient. Res.* **29**, 241–258.

LADING, L. 1971 Two-phase measurements utilizing laser-anemometer. Danish Atomic Research Energy Commission Research Establishement, Risö-M-1368.

LEE, S. L. & SRINIVANIN, J. 1978 Measurement of local size and velocity probability density distributions in two-phase suspension flows by laser Doppler technique. *Int. J. Multiphase Flow* **4**, 141–155.

LEE, S. L. &DURST, F. 1980 On the motion of particles in turbulent flows. SFB 80/TE/142-Rep, Univ. of Karlsruhe, F.R.G.

LISKA, J. J. 1979 The application of laser-Doppler anemometry to bubbly two-phase flows. M.A.Sc.-Thesis, Dep. of Mechanical Engineering, Univ. of Toronto, Toronto, Canada.

OHBA, K., KISHIMOTO, I. & OGASAWARA, M. 1977 Simultaneous measurements of local liquid velocity and void fraction in bubbly flows using a gas laser—I. Principles and measuring procedure. Technology Reports of the Osaka University, No. 1328, pp. 547–556—II. Local properties of turbulent bubbly flows. Technology Reports of the Osaka University, Vol. 27, No. 1358, pp. 229–238.

OHBA, K. & YUHARA, T. 1979 Velocity measurements of both phases in two-phase flow using laser-Doppler velocimeter. *Proc. IMEKO Symp. Flow Measurement and Control Industry*, Tokyo, Japan, November.

POPPER, J., ABUAF, N. & HETSRONI, G. 1975 Velocity measurements in a two-phase turbulent jet. *Int. J. Multiphase Flow* **1**, 715–726.

RIETHMÜLLER, M. L. 1973 Optical measurements of velocity in particulate flows. von Kármán Institute for Fluid Dynamics.

ROLANSKY, M. S., WEINBAUM, S. & PFEFFER, R. 1976 Drag reduction in dilute gas solid suspension flow: gas and particle velocity profiles. *3rd Int. Conf. Pneumatic Transport of Solids in Pipes*, Paper Cl, April.

STÜMKE, A. & UMHAUER, H. 1978 Local particle velocity distribution in two-phase flows measured by laser-Doppler velocimetry. *Proc. Dynamic Flow Conf.* 1978, Marseille and Baltimore, pp. 417–424, September.

UNGUT, A., YULE, A. J., CHIGIER, N. A. & ATAKAM, S. 1977 Particle size and velocity measurement by laser anemometry. *J. Energy* **1**, 220–228.

UNGUT, A., YULE, A. J., TAYLOR, D. S. & CHIGIER, N. A. 1978 Particle size measurement by laser anemometry. *J. Energy* **2**, 330–336.

WALLIS, G. B., 1974 The terminal speed of single drops or bubbles in an infinite medium. *Int. J. Multiphase Flow* **1**, 491–508.

WIGLEY, G. 1978 The sizing of large particles by laser anemometry. *J. Physics E.—Scient. Instr.* **11**, 639–642.